Inorg. Chem. **2003**, *42*, 8481–8488

Interpolymetallic Assembly of d^8–d^{10} Sulfide Aggregates from $[Pt_2(PPh_3)_4(\mu\text{-}S)_2]$ and Group 12 Metals

Zhaohui Li,† Weiming Zheng, Huang Liu, K. F. Mok, and T. S. Andy Hor*

Department of Chemistry, National University of Singapore, 3 Science Drive 3, Singapore 117543

Received July 25, 2003

A series of heterometallic Pt–M (M = Zn and Cd) sulfide aggregates with growing nuclearities $\{Pt_2M\}$, $\{Pt_4M\}$, and $\{Pt_4M_2\}$, viz., $[ZnPt_2Cl_2(PPh_3)_4(\mu_3\text{-}S)_2]$ (**2**), $[CdPt_2Cl_2(PPh_3)_4(\mu_3\text{-}S)_2]$ (**3**), $[Pt_2(PPh_3)_4(\mu_3\text{-}S)_2]_2[ZnSO_4]_2$ (**4**), $[Pt_2(PPh_3)_4(\mu_3\text{-}S)_2]_2[CdSO_4]_2\cdot H_2O$ (**5**), $[CdPt_4(PPh_3)_8(\mu_3\text{-}S)_4][ClO_4]_2$ (**7**), and $[ZnPt_4(PPh_3)_8(\mu_3\text{-}S)_4][ClO_4]_2$ (**8**), have been prepared from $Pt_2(PPh_3)_4(\mu\text{-}S)_2$ (**1**) with appropriate zinc and cadmium substrates. The structures have been determined by single-crystal X-ray diffraction. The supporting anions play an active role in the structural assembly process. An unexpected disintegration complex $[Pt_2(S_2CH_2)Cl(PPh_3)_4][PF_6]$ (**6**) has also been isolated and characterized by single-crystal X-ray diffraction. The mechanism of the formation of **6** is proposed.

Introduction

Our recent interest in d^8–d^n heterometallic chemistry based on the metalloligand $Pt_2(PPh_3)_4(\mu\text{-}S)_2$, **1**,[1] has led to the isolation of a variety of intermetallic sulfide aggregates of unusual structures.[1] However, the majority of these are limited to trinuclear $\{Pt_2M\}$ complexes because their formation is confined to 1/1 addition between the acidic [M] and basic **1**. Attempts to develop growing aggregates have insofar met with limited success, with the d^8–d^{10} system being among the notable exceptions in which we developed a chain of growing aggregates, viz., $Pt_2 \rightarrow Pt_2Ag \rightarrow Pt_2Ag_2 \rightarrow Pt_4Ag_2$.[2] Similar success, but to a less extent, was also experienced in the Pt^{II}/Au^I [3] and Pt^{II}/Hg^{II} [4] systems. This earlier promise prompted us to examine other d^8–d^{10} systems such as those with Zn(II) and Cd(II). These group 12 metals are of special interest because of their flexible geometry, high ligand mobility, and sulfur affinity, all of which are essential qualities for aggregate growth with **1**. The inherent d–p–s mix orbital nature makes this an ideal model in intermetallic studies. The current interest in thioenzymes,[5] heteronuclear FeZn cores in the active sites of purple acid[6] and human calcineurin,[7] and ^{113}Cd NMR[8] in metalloenzyme study are additional incentives for this work. Prior to our study, there were some but limited studies in Pt–Zn[9,10] and Pt–Cd[11] heterometallic chemistry.

We herein report the preparations of a series of intermetallic Pt–Zn and Pt–Cd sulfide aggregates with growing nuclearities, viz., $\{Pt_2M\}$, $\{Pt_4M\}$, and $\{Pt_4M_2\}$ (M = Zn, Cd), and demonstrate the active role that supporting or "spectator" anions can play in the structural assembly process. In the course of study, we came across an unexpected and unusual disintegration complex of a seemingly straightforward 1/1 addition product.

Results and Discussion

Complex **1** is sufficiently nucleophilic to capture binary compounds of M(II) (M = Zn, Cd) (Scheme 1) It adds to

* Author to whom correspondence should be addressed. E-mail: andyhor@nus.edu.sg.

† Current affiliation: Research Institute of Photocatalysis, Fuzhou University, Fuzhou, 350002, P. R. China.

(1) Fong, S. W. A.; Hor, T. S. A. *J. Chem. Soc., Dalton Trans*. **1999**, 639.
(2) Liu, H.; Tan, A. L.; Cheng, C. R.; Mok, K. F.; Hor, T. S. A. *Inorg. Chem.* **1997**, 36, 2916.
(3) (a) Li, Z.; Loh, Z.-H.; Mok, K. F.; Hor, T. S. A. *Inorg. Chem.* **2000**, *39*, 5299. (b) Li, Z.; Mok, K. F.; Hor, T. S. A. *J. Organomet. Chem.*, accepted.
(4) Li, Z.; Xu, X.; Khoo, S. B.; Mok, K. F.; Hor, T. S. A. *J. Chem. Soc., Dalton Trans.* **2000**, 2901.
(5) Stiefel, E. I.; George, G. N. *Bioinorganic Chemistry*, Bertini, I., Gray, H. B., Lippard, S. J., Valentine, J. S., Eds.; University Science Books: Mill Valley, CA, 1994; Chapter 7, pp 365–454.
(6) Sträter, N.; Klabunde, T.; Tucker, P.; Witzel, H.; Krebs, B. *Science* **1995**, *268*, 1489.
(7) Kissinger, C. R.; Parge, H. E.; Knighton, D. R.; Lewis, C. T.; Pelletier, L. A.; Tempczyk, A.; Kalish, V. J.; Tucker, K. D.; Showalter, R. E.; Moomaw, E. W.; Gastinel, L. N.; Habuka, N.; Chen, X.; Maldonado, F.; Barker, J. E.; Bacquet, R.; Villafranca, J. E. *Nature (London)* **1995**, *378*, 641.
(8) Armitage, I. M.; Schoot Uiterkamp, A. J. M.; Chlebowski, J. R.; Coleman, J. E. *J. Magn. Reson.* **1978**, *29*, 375.
(9) Poat, J. C.; Slawin, A. M. Z.; Williams, D. J.; Woollins, J. D. *J. Chem. Soc., Chem. Commun.* **1990**, 1036.
(10) Schöllhorn, H.; Thewalt, U.; Lippert, B. *Inorg. Chim. Acta* **1985**, 108, 77.
(11) Pettinari, C.; Marchetti, F.; Cingolani, A.; Troyanov, S. I.; Drozdov, A. *J. Chem. Soc., Dalton Trans.* **1998**, 3335.

10.1021/ic034884+ CCC: $25.00
Published on Web 11/06/2003

Scheme 1. Preparations of Complexes **2**−**8**

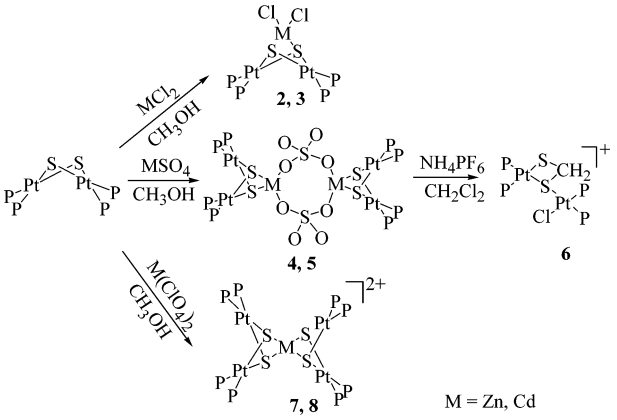

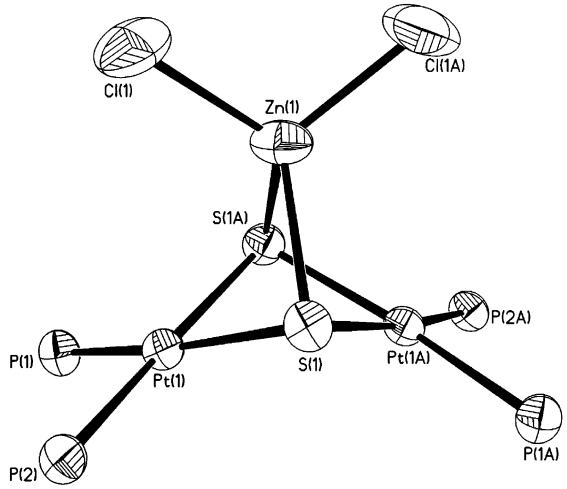

Figure 1. Thermal ellipsoid plot (50% probability) of $[ZnPt_2Cl_2(PPh_3)_4(\mu_3\text{-}S)_2]$, **2** (phenyl rings omitted for clarity).

$ZnCl_2$ stoichiometrically to give a 1/1 addition product $[ZnPt_2Cl_2(PPh_3)_4(\mu_3\text{-}S)_2]$, **2**, that is electrostatically neutral. Its formation signals a simple access to a trimetallic complex with a rare $\{ZnPt_2S_2\}$ chromophore. Its $^{31}P\{^1H\}$ NMR spectrum gives a single resonance (δ 19.9 ppm), thus suggesting chemical equivalence of all four phosphines. It also points to a nonmigratory model of phosphines on the MPt_2 triangle. The local geometries of this heterometallic triangle are revealed in a single-crystal X-ray diffraction analysis (Table 1 and Figure 1). A symmetric chelation of the $\{Pt_2S_2\}$ metalloligand at the Zn(II) center has resulted in a metal triangle with a tetrahedral Zn(II) and two square planar Pt(II). Solution studies do not support any cross-metal ligand migration, as opposed to the related d^8-d^8 systems.[12] The heterometals are within close proximity (Zn···Pt [av 3.092(2) Å]; Pt···Pt [3.250(2) Å]), but these do not justify direct M−M bonding. The Zn−S bonds [av 2.418(2) Å] are significantly longer than those in typical Zn−thiol adducts, e.g., [Zn(dtsq)(batho)] [2.317 Å] (dtsq = dithiosquarate, batho = 2,9-dimethyl-4,7-diphenyl-1,10-phenanthroline)[13] and $[Zn_2(i\text{-}MNT)_2(4\text{-}mpy)_4\cdot CHCl_3]$ [2.317−2.321 Å] (i-MNT = 1,1-dicyanoethylene-2,2-dithiolate, 4-mpy = 4-methylpyridine),[14] but the Zn−Cl bonds [av 2.244(2) Å] are fairly typical (cf. Zn−Cl in $ZnCl_2(C_4H_8N_2S_2)$ [2.240(1) Å]).[15] The significantly different stereogeometric demands of the ligands on Zn(II) force it to take up a distorted tetrahedral form with two contrasting L−M−L angles [Cl(1)−Zn(1)−Cl(1A), 108.9(2)°, and S(1)−Zn(1)−S(1A), 79.00(8)°].

Similarly a 1/1 adduct $[CdPt_2Cl_2(PPh_3)_4(\mu_3\text{-}S)_2]$, **3**, could also be obtained in an equimolar mixture of **1** and $CdCl_2$. The phosphines are equivalent, as evident in the $^{31}P\{^1H\}$ NMR spectrum (δ 21.1 ppm). X-ray study revealed an isostructural $[CdPt_2]$ triangle with phosphines on Pt(II) and chlorides completing a distorted tetrahedral environment at Cd(II) (Table 1). To accommodate a bigger metal (Cd) (and longer M−L bonds), the S−M−S chelate angle contracts further from 79.00(8)° [S(1)−Zn−S(1A)] in **2** to 72.77(6)° [S(1)−Cd(3)−S(2)] in **3**. This leads to more distortion from ideal tetrahedral geometry at Cd(II). Cd−S [av 2.645(2) Å] and Cd−Cl bonds [av 2.496 (3) Å] are comparable to those found in $CdCl_3\{Co(aet)_2(en)\}(Tbp)$ [av 2.662 (2) Å and av 2.495(2) Å, respectively] (aet = 2-aminoethanethiolate, en = ethylenediamine).[16] The covalent Zn−S and Cd−S bonds in **2** and **3** support the stability of these two complexes. Our previous results show that reacting **2** or **3** with bipy can lead to cationic $[MPt_2Cl(PPh_3)_4(\mu_3\text{-}S)_2(bipy)][PF_6]$ (M = Zn, Cd).[17] Unlike their Co analogue $[CoPt_2Cl_2(PPh_3)_4(\mu_3\text{-}S)_2]$,[18] complexes **2** and **3** are inert to desulfurization under CO conditions. Compared to Zn···Pt [av 3.092 Å] in **2**, the Cd···Pt separation [av 3.324 Å] necessarily increases. The basic $\{Pt_2S_2\}$ core does not need to make significant adjustment in order to accommodate a bigger metal. This is exemplified in the similar Pt···Pt [3.311(2) Å in **3** vs 3.250(2) Å in **2**] and S···S [3.138(2) Å in **3** vs 3.076(2) Å in **2**] distances. This explains how **1** can adapt to a variety of heterometals and geometries. The tunable dihedral angle between the two Pt planes also plays a key role in supporting the intermetallic aggregate assembly.[19,20] Recent studies suggested that the two planes open, resulting in a flattened butterfly, with the increasing size of the heterometal and longer M−S lengths.[20] Comparison of **2**, **3**, and the similar Co(II) adduct $[CoPt_2Cl_2(PPh_3)_4(\mu_3\text{-}S)_2]$[18] further substantiates this dihedral angle vs size relationship in this series: Cd (1.48 Å;[21] 132.2°) > Zn (1.31 Å;[21] 130.5°) > Co (1.25 Å;[21] 127.9°).

An equimolar amount of $ZnSO_4$ and **1** in MeOH gives a clear solution **4a**, from which yellow crystals characterized as $[Pt_2(PPh_3)_4(\mu_3\text{-}S)_2ZnSO_4]_n$, **4b**, are obtained. These crystals have poor solubility in MeOH. Molar conductivity measurement in CH_2Cl_2 suggests a nonelectrolyte, but in MeOH,

(12) Yeo, J. S. L.; Li, G.; Yip, W. H.; Henderson, W.; Mak, T. C. W.; Hor, T. S. A. *J. Chem. Soc., Dalton Trans.* **1999**, 435.
(13) Gronlund, P. J.; Burt, J. A.; Wacholtz, W. F. *Inorg. Chim. Acta* **1995**, *234*, 13.
(14) Xiong, R.-G.; Zuo, J.-L.; You, X.-Z. *Inorg. Chem.* **1997**, *36*, 2472.
(15) Antolini, L.; Fabretti, A. C.; Franchini, G.; Menabue, L.; Pellacani, G. C.; Desseyn, H. D.; Dommisse, R.; Hofmans, H. C. *J. Chem. Soc., Dalton Trans.* **1987**, 1921.
(16) Konno, T.; Okamoto, K. *Chem. Lett.* **1996**, 975.
(17) Li, Z.; Loh, Z.-H.; Fong, S. W. A.; Yan, Y.-K.; Henderson, W.; Mok, K. F.; Hor, T. S. A. *J. Chem. Soc., Dalton Trans.* **2000**, 1027
(18) Liu, H.; Tan, A. L.; Mok, K. F.; Hor, T. S. A. *J. Chem. Soc., Dalton Trans.* **1996**, 4023.
(19) Capdevila, M.; Clegg, W.; González-Duarte, P.; Jarid, A.; Lledós, A. *Inorg. Chem.* **1996**, *35*, 490.
(20) Tan, A. L.; Chiew, M. L.; Hor, T. S. A. *J. Mol. Struct. (THEOCHEM)* **1996**, *393*, 189.
(21) Sanderson, R. T. *Chemical Periodicity*; Reinhold: New York, 1996.

Table 1. Selected Bond Lengths (Å) and Bond Angles (deg) for **2**−**7**

(1) $[ZnPt_2Cl_2(PPh_3)_4(\mu_3\text{-}S)_2]\cdot H_2O$ (**2**)

Pt(1)−P(2)	2.277(2)	Pt(1)−P(1)	2.293(2)
Pt(1)−S(1)	2.352(2)	Pt(1)−S(1A)	2.378(2)
Zn(1)−Cl(1A)	2.244(2)	Zn(1)−Cl(1)	2.244(2)
Zn(1)−S(1A)	2.418(2)	Zn(1)−S(1)	2.418(2)
Pt(1A)−S(1)	2.378(2)	Zn(1)···Pt(1A)	3.092(1)
Zn(1)···Pt(1)	3.092(1)	Pt(1)···Pt(1A)	3.250(2)
S(1)···S(1A)	3.076(2)		
dihedral angle	130.5		
P(2)−Pt(1)−P(1)	98.73(6)	S(1)−Pt(1)−S(1A)	81.13(6)
Cl(1)−Zn(1)−Cl(1A)	108.90 (2)	Cl(1)−Zn(1)−S(1)	116.58(8)
Cl(1A) −Zn(1)−S(1)	116.72(8)	Cl(1)−Zn(1)−S(1A)	116.72(8)
Cl(1A) −Zn(1)−S(1A)	116.58(8)	S(1)−Zn(1)−S(1A)	79.00(8)

(2) $[CdPt_2Cl_2(PPh_3)_4(\mu_3\text{-}S)_2]\cdot CH_2Cl_2\cdot H_2O$ **(3)**

Pt(1)−P(2)	2.314(2)	Pt(1)−P(1)	2.337(2)
Pt(1)−S(2)	2.389(2)	Pt(1)−S(1)	2.417(2)
Pt(2)−P(3)	2.336(2)	Pt(2)−P(4)	2.314(2)
Pt(2)−S(2)	2.416(2)	Pt(2)−S(1)	2.387(2)
Cd(3)−S(2)	2.644(2)	Cd(3)−S(1)	2.646(2)
Cd(3)−Cl(1)	2.496(3)	Cd(3)−Cl(2)	2.497(3)
Pt(1)···Cd(3)	3.320(1)	Pt(2)···Cd(3)	3.328(1)
Pt(1)···Pt(2)	3.311(2)	S(1)···S(2)	3.138(2)
dihedral angle	132.2		
P(2)−Pt(1)−P(1)	99.41(7)	P(4)−Pt(2)−P(3)	98.79(7)
S(1)−Pt(2)−S(2)	81.59(6)	S(2)−Cd(3)−S(1)	72.77(6)
Cl(1)−Cd(3)−Cl(2)	107.58(11)	Cl(1)−Cd(3)−S(2)	119.55(9)
Cl(2)−Cd(3)−S(2)	118.16(8)	Cl(1)−Cd(3)−S(1)	117.43(9)
Cl(2)−Cd(3)−S(1)	118.44(9)		

(3) $[Pt_2(PPh_3)_4(\mu_3\text{-}S)_2]_2[ZnSO_4]_2\cdot CH_3OH\cdot H_2O$ **(4)**

Pt(1)−P(1)	2.280(2)	Pt(1)−P(2)	2.296(2)
Pt(1)−S(1)	2.365(2)	Pt(1)−S(2)	2.370(2)
Pt(2)−P(3)	2.299(2)	Pt(2)−P(4)	2.303(2)
Pt(2)−S(1)	2.354(2)	Pt(2)−S(2)	2.384(2)
Zn(3)−S(1)	2.396(2)	Zn(3)−S(2)	2.388(2)
Zn(3)−O(34)	1.932(6)	Zn(3)−O(31)	1.932(7)
S(3)−O(31)	1.409(7)	S(3)−O(34A)	1.400(7)
S(3)−O(33)	1.431(12)	S(3)−O(32)	1.434(7)
Pt(1)···Zn(3)	3.062(1)	Pt(2)···Zn(3)	3.143(1)
Pt(1)···Pt(2)	3.215(1)	S(1)···S(2)	3.068(1)
Zn(1)···Zn(2)	4.553(1)		
P(1)−Pt(1)−P(2)	99.96(6)	P(3)−Pt(2)−P(4)	102.07(6)
S(1)−Pt(2)−S(2)	80.73(5)	S(1)−Pt(1)−S(2)	80.78(5)
O(34)−Zn(3)−O(31)	110.1(4)	O(34)−Zn(3)−S(2)	121.6(4)
O(31)−Zn(3)−S(2)	113.9(3)	O(34)−Zn(3)−S(1)	113.4(2)
O(31)−Zn(3)−S(1)	115.1(3)	S(2)−Zn(3)−S(1)	79.80(6)
O(34A) −S(3)−O(33)	101.9(8)	O(31)−S(3)−O(33)	109.2(9)
O(34A) −S(3)−O(32)	110.0(5)	O(31)−S(3)−O(32)	110.2(5)
O(33)−S(3)−O(32)	111.9(8)	S(3)−O(31)−Zn(3)	146.0(5)
S(3A) −O(34)−Zn(3)	151.6(6)		

(4) $[Pt_2(PPh_3)_4(\mu_3\text{-}S)_2]_2[CdSO_4]_2\cdot 4CH_3OH\cdot 2H_2O$ **(5)**

Pt(1)−P(1)	2.297(1)	Pt(1)−P(2)	2.303(2)
Pt(1)−S(1)	2.347(1)	Pt(1)−S(2)	2.378(2)
Pt(2)−P(3)	2.277(2)	Pt(2)−P(4)	2.291(2)
Pt(2)−S(1)	2.352(2)	Pt(2)−S(2)	2.363(2)
Cd(3)−S(1)	2.649(2)	Cd(3)−S(2)	2.574(2)
Cd(3)−O(1)	2.200(5)	Cd(3)−O(2)	2.221(7)
Cd(3)−O(5)	2.427(10)	S(3)−O(2)	1.431(7)
S(3)−O(1A)	1.488(6)	S(3)−O(3)	1.426(7)
S(3)−O(4)	1.465(8)	O(1)−S(3A)	1.488(6)
Pt(1)···Cd(3)	3.321(1)	Pt(2)···Cd(3)	3.232(1)
P(1)−Pt(1)−P(2)	101.87(5)	P(3)−Pt(2)−P(4)	100.85(6)
S(1)−Pt(2)−S(2)	81.77(5)	S(1)−Pt(1)−S(2)	81.56(5)
O(1)−Cd(3)−O(2)	104.0(3)	O(1)−Cd(3)−O(5)	87.1(3)
O(2)−Cd(3)−O5)	83.2(4)	O(1)−Cd(3)−S(2)	135.47(19)
O(2)−Cd(3)−S(2)	120.3(2)	O(5)−Cd(3)−S(2)	94.0(2)
O(1)−Cd(3)−S(1)	105.26(16)	O(2)−Cd(3)−S(1)	100.0(2)
O(5)−Cd(3)−S(1)	165.8(2)	S(2)−Cd(3)−S(1)	72.42(5)
S(3)−O(2)−Cd(3)	134.2(4)	O(3)−S(3)−O(2)	111.2(5)
O(3)−S(3)−O(4)	110.2(5)	O(2)−S(3)−O(4)	108.9(7)
O(3)−S(3)−O(1A)	110.3(4)	O(2)−S(3)−O(1A)	108.6(4)
O(4)−S(3)−O(1A)	107.5(5)	S(3A)−O(1)−Cd(3)	133.5(4)

(5) $[Pt_2(S_2CH_2)Cl(PPh_3)_4][PF_6]$ (**6**)

Pt(1)−P(1)	2.265(3)	Pt(1)−P(2)	2.324(3)
Pt(1)−Cl(1)	2.327(3)	Pt(1)−S(1)	2.389(3)
Pt(2)−P(4)	2.296(3)	Pt(2)−P(3)	2.303(4)
Pt(2)−S(2)	2.321(4)	Pt(2)−S(1)	2.382(3)
S(1)−C(73)	1.805(15)	S(2)−C(73)	1.783(14)
Pt(1)···Pt(2)	3.960(3)	S(1)···S(2)	2.837(3)
P(1)−Pt(1)−P(2)	95.27(12)	P(1)−Pt(1)−Cl(1)	178.06(14)
P(2)−Pt(1)−Cl(1)	85.17(12)	P(1)−Pt(1)−S(1)	91.51(11)
P(2)−Pt(1)−S(1)	173.13(11)	Cl(1)−Pt(1)−S(1)	88.09(11)
P(4)−Pt(2)−P(3)	102.71(12)	P(4)−Pt(2)−S(2)	88.65(13)
P(3)−Pt(2)−S(2)	167.54(13)	P(4)−Pt(2)−S(1)	162.77(12)
P(3)−Pt(2)−S(1)	94.26(12)	S(2)−Pt(2)−S(1)	74.19(13)
S(2)−C(73)−S(1)	104.5(7)	Pt(2)−S(1)−Pt(1)	112.18(12)

(6) $[CdPt_4(PPh_3)_8(\mu_3\text{-}S)_4][ClO_4]_2\cdot 5CH_2Cl_2\cdot H_2O$ (**7**)

Pt(1)−P(2)	2.285(2)	Pt(1)−P(1)	2.311(2)
Pt(1)−S(1)	2.361(2)	Pt(1)−S(1A)	2.379(2)
Pt(2)−P(4)	2.292(2)	Pt(2)−P(3)	2.309(3)
Pt(2)−S(2A)	2.359(2)	Pt(2)−S(2)	2.377(2)
Cd(3)−S(2A)	2.590(2)	Cd(3)−S(2)	2.590(2)
Cd(3)−S(1A)	2.596(2)	Cd(3)−S(1)	2.596(2)
S(1)−Pt(1A)	2.379(2)	S(2)−Pt(2A)	2.359(2)
Pt(1)···Cd(3)	3.257(2)	Pt(2)···Cd(3)	3.256(2)
Pt(1)···Pt(1A)	3.253(2)	Pt(2)···Pt(2A)	3.264(2)
S(1)···S(1A)	3.111(2)	S(2)···S(2A)	3.095(2)
P(2)−Pt(1)−P(1)	97.22(8)	P(4)−Pt(2)−P(3)	97.33(9)
S(2A) −Pt(2)−S(2)	81.62(8)	S(1)−Pt(1)−S(1A)	82.03(8)
S(2A)−Cd(3)−S(2)	73.40(10)	S(2A)−Cd(3)−S(1A)	116.60(7)
S(2)−Cd(3)−S(1A)	146.74(6)	S(2A)−Cd(3)−S(1)	146.74(6)
S(2)−Cd(3)−S(1)	116.60(7)	S(1A) −Cd(3)−S(1)	73.60(9)

partial ionization occurs. The $^{31}P\{^1H\}$ NMR spectrum in CD_2Cl_2 gives equivalent phosphines (δ 20.3 ppm). These data are consistent with a neutral adduct as seen in **2** and **3**, but give no affirmative information on nuclearity. Subsequent X-ray single-crystal diffraction analysis shows an unusual and unexpected fused-macrocylic structure comprising an eight-membered $\{Zn_2S_2O_4\}$ ring sandwiched between two metallocyclic rings of $\{Pt_2ZnS_2\}$ (Table 1 and Figure 2). This is a result of two Zn(II) chelated by **1** and doubly bridged by sulfate. This overall Pt_4Zn_2 structure has a crystallographically imposed center of symmetry. Effectively, the open-bridging sulfate allows the trimetal core in **2** and **3** to dimerize and give a hexametallic core here. This dimerization was not expected since sulfate chelation, and hence production of a complex like $[Pt_2(PPh_3)_4(\mu_3\text{-}S)_2(ZnSO_4)]$, is known. It could not be sustained here because of the acute strain that would be imposed on the $[Zn(O_2SO_2)]$ chelate ring. Intermolecluar dimerization provides a facile pathway to relieve such a chelate and replace it with a geometrically more adaptable double-bridge structure. This results in a near-tetrahedral angle for $\angle$O−Zn−O [av 110.1(4)°] for Zn(II), which lends stabilization to **4**. Surprisingly, although Zn(II)

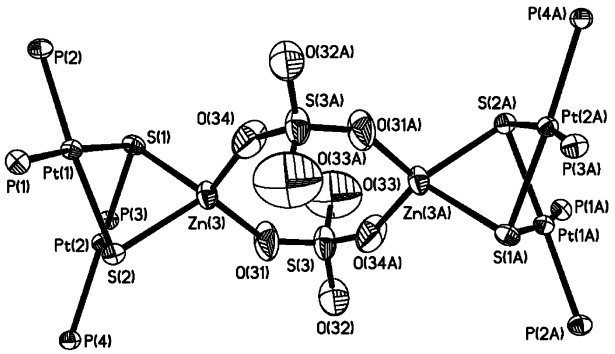

Figure 2. Thermal ellipsoid plot (30% probability) of $[Pt_2(PPh_3)_4(\mu_3\text{-}S)_2]_2[ZnSO_4]_2$, **4** (phenyl rings and solvates omitted for clarity).

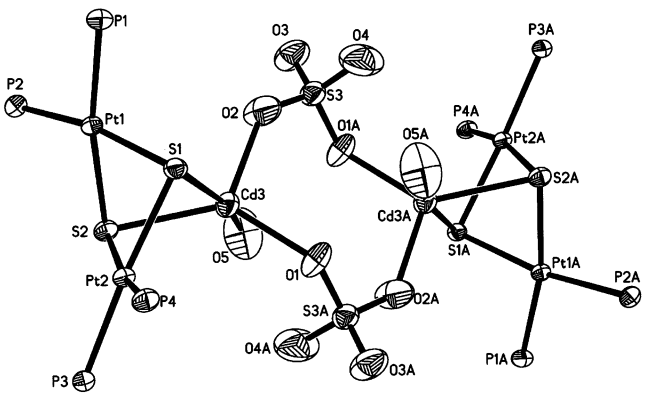

Figure 3. Thermal ellipsoid plot (50% probability) of $[Pt_2(PPh_3)_4(\mu_3\text{-}S)_2]_2[CdSO_4]_2$, **5** (phenyl rings and solvates omitted for clarity).

is known to be oxophilic, there are very few structurally characterized Zn(II) complexes with coordinating SO_4^{2-}. For those that are reported, the ligand is almost invariably monodentate. This is therefore a rare sulfato-bridged Zn(II) dimer and one of the few reported.[22,23] The four O atoms in this eight-membered-ring $\{Zn_2O_4S_2\}$ could define a plane, with the two metal (Zn) nearly coplanar (±0.0725 Å from plane) and two S atoms slightly displaced above and below (±0.413 Å). Accordingly, the two sets of terminal oxygen on sulfur are pointing in opposite directions away from the Zn_2O_4 plane. As expected, the two Zn atoms are nonbonding [4.553 Å]. This hexametallic arrangement was earlier witnessed in $[Pd_2Pt_4(\mu_2\text{-}Cl)_2(\mu_3\text{-}S)_4(PPh_3)_8][PF_6]_2$[24] except that the latter is supported by a much more common chloro bridge at the center.

The Zn−S bonds [2.369(2) Å] in **4** are comparable to those in **2** [2.418(2) Å]. The Zn−O bonds [av 1.932(6) Å] are comparable to those in a similar sulfato-bridged dimer $[Zn_2(SO_4)_2L_2]$ (tetrahedral) ([L = 2,9-dimethyl-1,10-phenanthroline] [1.926(2) Å]),[22] but shorter than those in $ZnL_2(SO_4)$ (L = 1,2-ethanediol) (octahedral) [2.067(3) Å].[25] The $S-O_{coordinated}$ lengths [av 1.405(7) Å] are unexpectedly short (compared to 1.476−1.513 Å in other dimers), and the $S-O_{free}$ lengths [av 1.433 Å] are normal (cf. 1.437−1.464 Å).[22,23] These fairly indistinguishable $S-O_{coordinated}$ and $S-O_{free}$ bonds could be attributed to the delocalization effect.

Analogous reaction of **1** with an equimolar amount of $CdSO_4$ in MeOH also leads to a clear solution **5a**, from which a similar Cd analogue $[Pt_2(PPh_3)_4(\mu_3\text{-}S)_2CdSO_4]_n$, **5b**, is obtained**.** The phosphines are equivalent (δ_P 21.1 ppm). It easily dissolves in CH_2Cl_2 and gives a nonelectrolyte, but, similar to **4b**, it has limited solubility in MeOH and shows some degree of ionization. X-ray diffraction analysis gave the expected hexametallic core with double-bridging sulfate (as in **4**) but with some additional unexpected features (Table 1 and Figure 3). Each Cd(II) captures an aqua ligand [Cd−O, 2.427(10) Å] to give a 5-coordinate structure. The aqua oxygen and a sulfur atom take up the axial positions [O(5)−Cd−S(1), 165.8(2)°] whereas the sulfate oxygen and the remaining sulfur occupy the equatorial positions, thus completing a distorted tbp local geometry. The equatorial−equatorial and axial−equatorial angles range from 104.0(3)° to 135.47(19)° and from 72.42(5)° to 105.26(16)°, respectively. This, to our knowledge, is the first structurally characterized sulfato-bridged Cd(II) dimer, amidst the several Cd(II) sulfate complexes known.[26] The different metal (Cd) geometry entails a different ring conformation in order to minimize interligand repulsions. (Figure 4). To avoid the axial ligands protruding into the center of the molecule where the sulfate is located, the metals are deviated from the O_4 (±0.9867 Å) and instead the sulfur atoms are much closer to this plane (±0.4673 Å). Effectively the sulfur and metal swap positions in the two conformations, thereby minimizing interactions between the terminal oxygen at the bridge with the metalloligands on the metal (Zn/Cd).

The crystalline samples of **4** and **5** used for crystallographic elucidation have limited solubility in MeOH whereas the precrystallization samples **4a** and **5a** are readily soluble. Conductivity measurement of saturated MeOH solution of **4** and **5** ($\sim 10^{-4}$ mol·dm^{-3}) shows that they undergo dissociation in MeOH. These give peripheral evidence that the solid-state structures could be different from that of the solution state. Since there is no evidence to suggest chemical change, the most likely possibility is the formation of nuclearity isomers. The primary products (**4a** and **5a**) could be mononuclear complexes with chelating sulfate, which dissociates in MeOH. Upon recrystallization, the sulfate re-enters the coordination sphere as a bridge, thus resulting in the dinuclear structures in **4** and **5** (Scheme 2). In an effort to understand this dynamic process better, we attempted a metathesis exchange of **4a** or **5a** (in MeOH) with NH_4PF_6. However, this resulted in an unexpected disintegration product, viz., $[Pt_2(S_2CH_2)Cl(PPh_3)_4][PF_6]$, **6**. Its peculiar and unique chemical identity was first revealed when its $^{31}P\{^1H\}$ NMR spectrum showed four discrete chemical environments (δ_P 22.9, 20.1, 19.8, and 14.2 ppm). Conductivity measurement supports a 1:1 electrolyte in CH_2Cl_2. Subsequent X-ray crystallographic data confirms that

(22) Harvey, M.; Baggio, S.; Mombru, A.; Baggio, R. *Acta Crystallogr.* **2000**, *C56*, 771.
(23) Katsoulakou, E.; Lalioti, N.; Raptopoulou, C. P.; Terzis, A.; Manessi-Zoupa, E.;. Perlepes, S. P. *Inorg. Chem. Commun.* **2002**, *5*, 719.
(24) Briant, C. E.; Hor, T. S. A.; Howells, N. D.; Mingos, D. M. P. *J. Chem. Soc., Chem. Commun.* **1983**, 1118.
(25) Labadi, I.; Parkanyi, L.; Kenessey, G.; Liptay, G. *J. Crystallogr. Spectrosc. Res.* **1993**, *23*, 333.
(26) Plater, M. J.; Foreman, M. R. St. J.; Gellbrich, T.; Coles, S. J.; Hursthouse, M. B. *J. Chem. Soc., Dalton Trans.* **2000**, 3065.

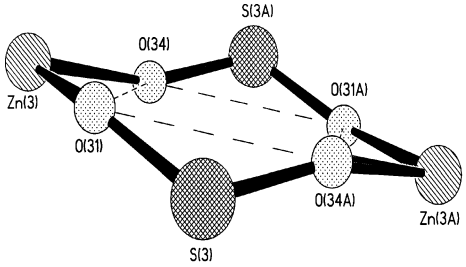

4

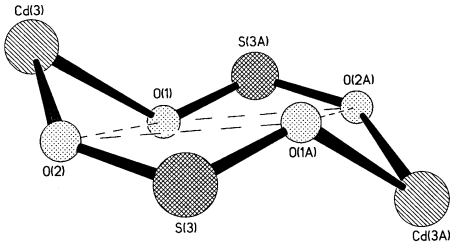

5

Figure 4. Eight-membered rings found in **4** and **5**.

Scheme 2. Formation of $\{M_2O_4S_2\}$ from $\{MO_2S\}$ through Dimerization

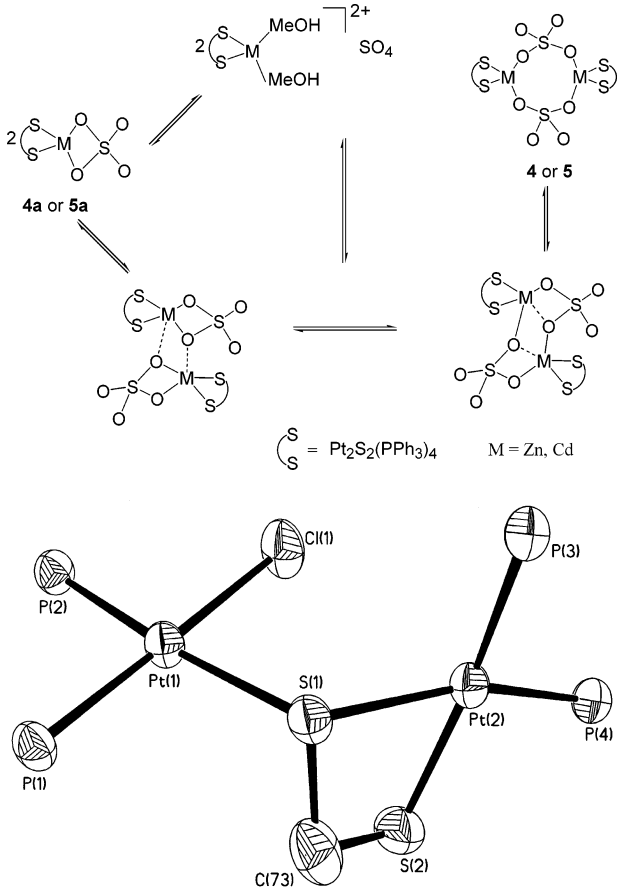

Figure 5. Thermal ellipsoid plot (50% probability) of $[Pt_2(S_2CH_2)Cl(PPh_3)_4]^+$, (**6**) (phenyl rings omitted for clarity).

the sulfate ligands are displaced, but there are secondary changes (Table 1 and Figure 5). The $\{Pt_2S_2\}$ core has disintegrated into a cationic $\{Pt_2(S_2CH_2)\}$ moiety. Effectively, the two μ_2-sulfide ligands have transformed to a μ,η-methanedithiolate ligand, which serves to connect the two Pt(II) centers. Apart from the phosphines, a chloride has entered the coordination core. Although methanedithiolate is known in a few Pt(II) complexes, viz., $[Pt(S_2CH_2)(PMe_2Ph)_2]$[27] (**I**), $[Pt(S_2CH_2)(dppy)_2]$[28] (**II**), and $[Pt(S_2CH_2)(dppp)]$[29] (**III**), complex **6** is the only crystallographically proven

Table 2. Comparison of the Bond Lengths (Å) and Bond Angles (deg) of $[Pt_2(S_2CH_2)Cl(PPh_3)_4][PF_6]$ (**6**), $[Pt(S_2CH_2)(PMe_2Ph)_2]$ (**I**), $[Pt(S_2CH_2)(dppy)_2]$(**II**), and $[Pt(S_2CH_2)(dppp)_2]$(**III**)

	6	**I**	**II**	**III**
Pt−S	2.382	2.30	2.31	2.32
	2.321			
Pt−P	2.30	2.25	2.27	2.26
C−S	1.807	1.83	1.82	1.84
	1.783			
S−C−S	104.5	102.1	103.0	103.4
P−Pt−P	102.7	94.3	100.6	92.2
S−Pt−S	74.2	76.1	76.2	76.9

diplatinum methanedithiolate structure. A comparison of some key structure parameters of these complexes is given in Table 2. The presence of two chemically different sulfur sites in **6** leads to two significantly different Pt−S lengths [Pt(2)−S(2) 2.321(4) Å vs Pt(2)−S(1) 2.382(3) Å]. The S(1)→Pt(1) dative donation understandably weakens the S(1)−Pt(2) bond. The two P−Pt−P angles [95.27(12)° and 102.71(12)°] are also significantly different, which could be ascribed to the highly skewed asymmetric structure. The contrasting trans influence of Cl and S gives rise to significantly different Pt−P lengths [Pt(1)−P(1) 2.265(3) Å vs Pt(1)−P(2) 2.324(3) Å). As a chelate bridge, the dithiolate forces an acute angle [74.19(13)°] on a square-planar metal Pt(2). These distortions however do not have any apparent impact on the bond parameters in the $\{PtS_2C\}$ ring.

Similar reactions between **4a** or **5a** and NH_4BPh_4 led to an analogue of **6** with $[BPh_4]^-$ as counteranion. Formation of **6** from **4a** or **5a** is unexpected but can be understood (Scheme 3). Complex **4a** metathesizes with NH_4PF_6 or NH_4BPh_4, and entry of solvate (MeOH) to the coordinating sphere would yield $[(PPh_3)_4Pt_2(\mu_3\text{-}S)_2Zn(MeOH)_2][PF_6]_2$ (**A**), which decomposes in CH_2Cl_2 to give $[Pt_2(\mu\text{-}S)(\mu\text{-}SCH_2Cl)(PPh_3)_4]Cl$ (**B**) and then $[Pt_2(\mu\text{-}S_2CH_2)(PPh_3)_4]Cl_2$ (**C**). Both **B** and **C** are common thermodynamic products arising from nucleophilic attack of CH_2Cl_2 on the basic sulfur sites of $\{Pt_2S_2\}$.[30] Bridge cleavage of **C** to give $[Pt(S_2CH_2)(PPh_3)_2]$, **D** and $PtCl_2(PPh_3)_2$ is known.[31] Analogues of **D** have been reported by several teams.[27,28,29] Re-entering of $PtCl_2(PPh_3)_2$

(27) Shaver, A.; Lai, R. K.; Bird, P. H.; Wickramasinghe, W. *Can. J. Chem.* **1985**, *63*, 2555
(28) Yam, V. W. W.; Yeung, P. K. Y.; Cheung, K. K. *J. Chem. Soc., Chem. Commun.* **1995**, 267.
(29) Mas-Ballesté, R.; Capdevila, M.; Champkin, P. A.; Clegg, W.; Coxall, R. A.; Lledós, A.; Mégret, C.; González-Duarte, P. *Inorg. Chem.* **2002**, *41*, 3218.
(30) Briant, C. E.; Gardner, C. J.; Hor, T. S. A.; Howells, N. D.; Mingos, D. M. P. *J. Chem. Soc., Dalton Trans.* **1984**, 2645.
(31) Li, Z.; Fong, S. W. A.; Yeo, J. S. L.; Henderson, W.; Mok, K. F.; Hor, T. S. A. In *Modern Coordination Chemistry*; Leigh, G. F., Winterton, N., Eds.; 2002; pp 355−365.

Scheme 3. Proposed Mechanism for the Formation of **6**

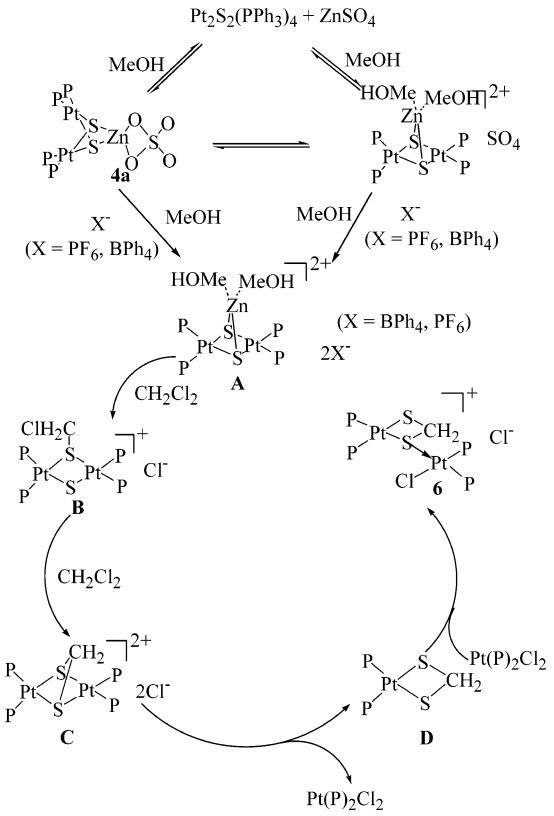

would neutralize the basic sulfur site of **D**. When this is followed by chloride dissociation, the observed product **6** therefore forms. Isolation of **6** thus provides evidence that the sulfur sites of **D** are sufficiently basic to function as a precursor to other heterometallic products. This would be a subject of our future studies.

To understand the role of ligands played in these unusual assemblies, we also attempted to use "ligand-free" substrates such as $Cd(ClO_4)_2$. Under 2:1 molar ratios with **1**, a pentanuclear aggregate $[CdPt_4(PPh_3)_8(\mu_3\text{-}S)_4][ClO_4]_2$, **7**, results. The conductivity measurement suggests a 2:1 electrolyte in CH_2Cl_2. X-ray analysis shows a distorted tetrahedral Cd(II) dicationic complex stabilized by two $\{Pt_2S_2\}$ butterflies (Table 1 and Figure 6). Some prior examples of such assembly were found in $[M\{Pt_2(dppe)_2(\mu\text{-}S)_2\}]X_2$[32] (M = Zn, Cd and Hg) and $[Hg\{Pt_2(\mu\text{-}S)_2(PPh_3)_4\}_2][BPh_4]_2$,[4,24] the crystal structure of which was determined recently, and $[Cu\{Pt_2S_2(PPh_3)_4\}_2][PF_6]_2$, with its structure spectroscopically established.[33] The four Cd−S bond lengths [2.590(2)−2.596(2) Å] and the two chelate angles [73.40(10)° and 73.60(9)°] are remarkably constant, although the structure is distorted significantly from ideal tetrahedral (the interchelate angles [116.60(7)° and 146.74(16)°] being significantly different from the intrachelate ones [73.50(10)°]). Accordingly, the dihedral angle between the two S−Cd−S planes [122.8°] is significantly distorted from ideal [90°].

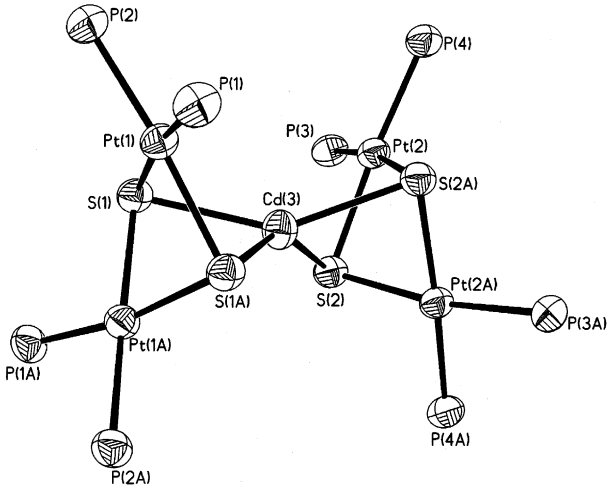

Figure 6. Thermal ellipsoid plot (50% probability) of $[CdPt_4(PPh_3)_8(\mu_3\text{-}S)_4]^{2+}$, **7** (phenyl rings omitted for clarity).

This distortion does not appear to affect the Cd−S strength [av 2.593(2) compared to 2.645(2) Å in **3**].

The asymmetric disposition of the two metalloligands around a distorted Cd(II) would suggest that, in the static state, the eight phosphine groups in **7** are not equivalent. The two peaks in the $^{31}P\{^1H\}$ NMR spectrum agree with this proposal (δ 20.6 ppm [^1J(P−Pt) = 3150] and 14.8 ppm [^1J(P−Pt) = 2995 Hz]). A similar phenomenon has been found in the Hg analogue $[Hg\{Pt_2(\mu_3\text{-}S)_2(PPh_3)_4\}_2][ClO_4]_2$, but not in $[Cu\{Pt_2S_2(PPh_3)_4\}_2][PF_6]_2$ or $[M\{Pt_2(dppe)_2(\mu_3\text{-}S)_2\}X_2$ (M = Zn, Cd and Hg).

Similar reaction between **1** and $Zn(ClO_4)_2$ in a 2:1 ratio leads to **8**, whose identity was established on the basis of spectroscopic, conductivity, and elemental analytical data as well as comparison with **7**. However, unlike **7**, the phosphines on **8** are equivalent (δ 14.3 ppm [^1J(P−Pt) = 3660]) at room temperature. This could be made possible by a facile twisting of the two butterflies on the central metal, which is faster than the NMR time scale.

The isolation of these heteropolymetallic compounds suggested that the spectator anions could play an active role in the structural assembly. When this is complemented by coordinative mobility of the ligand, geometrical variation of the metal, and the stereoconformational nonrigidity of the metalloligand, we have a system that has turned out to be remarkably complex. If we could understand, and harness, such complexity, we would be able to construct a series of growing heterometallics of novel, and quite often unusual and unexpected, structures. The isolation of $\{Pt_2M\}$, $\{Pt_4M_2\}$, and $\{Pt_4M\}$ (M = Zn, Cd) in this work epitomizes this approach. It also helps to direct our future target in polymetallic structural design.

Experimental Section

All reactions were routinely performed under a pure argon atmosphere unless otherwise stated. All solvents were distilled and degassed before use. $[Pt_2(PPh_3)_4(\mu\text{-}S)_2]$, **1**, was synthesized from *cis*-$[PtCl_2(PPh_3)_2]$ and $Na_2S\cdot 9H_2O$ according to a literature method.[34] Elemental analyses were conducted in the Elemental Analysis

(32) Capdevila, M.; Carrasco, Y.; Clegg, W.; Coxall, R. A.; González-Duate, P.; Lledós, A.; Ramírez, J. A. *J. Chem. Soc., Dalton Trans.* **1999**, 3103.

(33) Liu, H.; Tan, A. L.; Xu, Y.; Mok, K. F.; Hor, T. S. A. *Polyhedron* **1997**, *16*, 377.

(34) Ugo, R.; La Monica, G.; Cenimi, S.; Segre, A.; Conti, F. *J. Chem. Soc. A* **1971**, 522.

Table 3. Crystallographic Data and Structure Refinement for **2**−**7**

	2	**3**	**4**	**5**	**6**	**7**
chem formula	$C_{72}H_{62}Cl_2O$-$P_4Pt_2S_2Zn$	$C_{73}H_{64}Cl_4O$-$P_4Pt_2S_2Cd$	$C_{145}H_{126}O_{10}$-$P_8Pt_4S_6Zn_2$	$C_{148}H_{140}O_{14}$-$P_8S_6Pt_4Cd_2$	$C_{73}H_{62}ClF_6P_5Pt_2S_2$	$C_{150}H_{134}CdCl_{13}O_5$-$P_8Pt_4S_4$
fw	1659.67	1789.62	3379.68	3587.80	1697.83	3746.18
wavelength (Å)	0.71073	0.71073	0.71073	0.71073	0.71073	0.71073
T (K)	293(2)	293(2)	293(2)	293(2)	293(2)	293(2)
space group	P2/n	P-1	P2(1)/n	P2(1)/n	P2(1)/c	$C2/c$
a (Å)	17.427(2)	16.722(1)	18.372(1)	18.468(1)	10.562(3)	35.532(14)
b (Å)	11.567(2)	17.916(1)	17.756(1)	17.743(1)	31.801(1)	23.651(8)
c (Å)	17.635(2)	18.5601)	23.787(1)	23.874(1)	20.707(5)	26.660(13)
α (deg)		114.71(1)				
β (deg)	105.83(9)	102.94(1)	96.96(1)	97.38(1)	103.09(2)	123.65(2)
γ (deg)		97.95(1)				
vol (Å^3)	3420.1(9)	4751.14(7)	7702.33(14)	7758.18(13)	6774(3)	18651(13)
Z	2	2	2	2	4	4
D_{calc} (g cm^{-3})	1.610	1.251	1.457	1.531	1.665	1.334
μ (mm^{-1})	4.703	3.414	4.141	4.080	4.404	3.444
residuals: R_1,[a] wR_2[b]						
obs data	0.0340, 0.1117	0.0451, 0.1447	0.0371, 0.0.1155	0.0387, 0.1173	0.0555, 0.1172	0.0547, 0.1734
all data	0.0432, 0.1177	0.0605, 0.1577	0.0556, 0.1303	0.0549, 0.1294	0.1296, 0.1469	0.0911, 0.1982

[a] $R_1 = \sum||F_o| - |F_c||/\sum|F_o|$. [b] $wR_2 = \{\sum w[(F_o^2 - F_c^2)^2]/\sum wF_o^4\}^{1/2}$; $\rho = [(F_o^2,\theta) + 2F_c^2]/3$.

Laboratory in the Department of Chemistry. Conductivity was determined using a STEM conductivity 1000 m. The $^{31}P\{^1H\}$ NMR spectra were recorded on a Bruker ACF 300 spectrometer with H_3PO_4 as external reference.

Syntheses. (1) Synthesis of $[ZnPt_2Cl_2(PPh_3)_4(\mu_3\text{-}S)_2]$ (2). $ZnCl_2$ (0.013 g, 0.1 mmol) was added with stirring to a MeOH (40 cm^3) suspension of **1** (0.15 g, 0.1 mmol). After 6 h, the suspension, which changed gradually from orange to yellow, was filtered and the solid collected was purified by recrystallization in a CH_2Cl_2:MeOH (1:3) mixture to give yellow crystals of **2**·H_2O (0.106 g, 65%). Anal. Calcd for $C_{72}H_{60}Cl_2P_4Pt_2S_2Zn$: C, 52.75, H, 3.66, Cl, 4.33, P, 7.57, S, 3.91. Found: C, 52.34, H, 3.65, Cl, 4.17, P, 7.65, S, 3.97. $^{31}P\{^1H\}$ NMR (CD_2Cl_2): δ 19.9 ppm [t, ^1J(P−Pt) 3080 Hz].

(2) Synthesis of $[CdPt_2Cl_2(PPh_3)_4(\mu_3\text{-}S)_2]$ (3). Complex **3** was synthesized in a manner analogous to **2** from **1** (0.15 g, 0.1 mmol) and $CdCl_2$ (0.019 g, 0.1 mmol) in MeOH (30 cm^3). After 6 h, the yellow suspension was filtered and the yellow solid obtained was recrystallized in a CH_2Cl_2:MeOH (1:3) mixture to give yellow crystals of **3**·CH_2Cl_2·H_2O (0.106 g, 59%). Anal. Calcd for $C_{72}H_{60}$-$CdCl_2P_4Pt_2S_2$: C, 51.25, H, 3.56, P, 7.35, S, 3.80. Found: C, 50.76, H, 3.47, P, 7.24, S, 3.45. $^{31}P\{^1H\}$ NMR (CD_2Cl_2): δ 21.1 ppm [t, ^1J(P−Pt) 3010 Hz].

(3) Synthesis of $[Pt_2(PPh_3)_4(\mu_3\text{-}S)_2]_2[ZnSO_4]_2$ (4). $[Pt_2(PPh_3)_4$-$(\mu\text{-}S)_2]$, **1** (0.15 g, 0.1 mmol), was stirred with $ZnSO_4$·$7H_2O$ (0.028 g, 0.1 mmol) in MeOH (40 cm^3) for 2 h. Et_2O was added to the resultant clear yellow solution to give a yellow precipitate, which was recrystallized in MeOH to give yellow crystals of **4**·CH_3OH·H_2O (0.096 g, 56.8%). Anal. Calcd for $C_{144}H_{120}O_8P_8Pt_4S_6Zn_2$: C, 51.82, H, 3.60, P, 7.44, S, 5.76. Found: C, 51.26, H, 3.43, P, 7.65, S, 5.93. Λ_m ($\sim 10^{-4}$ mol dm^{-3}, MeOH, 55.0 Ω^{-1} cm^2 mol^{-1}). $^{31}P\{^1H\}$ NMR (CD_2Cl_2): δ 20.3 ppm [t, ^1J(P−Pt) 3080 Hz].

(4) Synthesis of $[Pt_2(PPh_3)_4(\mu_3\text{-}S)_2]_2[CdSO_4]_2$ (5). $[Pt_2(PPh_3)_4$-$(\mu\text{-}S)_2]$, **1** (0.15 g, 0.1 mmol) was stirred with $CdSO_4$·$8H_2O$ (0.026 g, 0.1 mmol) in MeOH (40 cm^3) for 2 h. Et_2O was added to the resultant clear yellow solution to give a yellow precipitate, which was recrystallized in MeOH to give yellow crystals of **5**·$4CH_3OH$·$2H_2O$ (0.087 g, 48.6%). Anal. Calcd for $C_{144}H_{120}O_8P_8Pt_4S_6Cd_2$: C, 50.50; H, 3.51; P, 7.25; S, 5.61. Found: C, 49.65; H, 3.61; P, 7.64; S, 5.34. Λ_m ($\sim 10^{-4}$ mol dm^{-3}, MeOH, 70.3 Ω^{-1} cm^2 mol^{-1}).$^{31}P\{^1H\}$ NMR (CD_2Cl_2): δ 21.1 ppm [t, ^1J(P−Pt) 2993 Hz].

(5) Synthesis of $[Pt_2(S_2CH_2)Cl(PPh_3)_4][PF_6]$ (6). $[Pt_2(PPh_3)_4$-$(\mu\text{-}S)_2]$ (0.10 g, 0.067 mmol) was stirred with $ZnSO_4$·$7H_2O$ (0.0191 g, 0.067 mmol) in MeOH (40 cm^3) for 2 h. The yellow solution was treated with NH_4PF_6 to give a yellow precipitate, which was recrystallized in CH_2Cl_2/hexane to give pale yellow crystals of **6** (0.0203 g, 17.9%). Anal. Calcd for $C_{73}H_{62}ClF_6P_5Pt_2S_2$: C, 51.60, H, 3.65, P, 9.13, S, 3.77. Found: C, 51.96, H, 3.45, P, 8.64, S, 4.01. Λ_m (10^{-3} mol dm^{-3}, CH_2Cl_2) 77.6 Ω^{-1} cm^2 mol^{-1}.$^{31}P\{^1H\}$ NMR (CD_2Cl_2): δ 22.9 ppm [t, ^1J(P−Pt) 3580 Hz], δ 20.1 ppm [t, ^1J(P−Pt) 2710 Hz], δ 18.3 ppm [t, ^1J(P−Pt) Hz, 3190 Hz], δ 13.3 ppm [t, ^1J(P−Pt) 3040 Hz].

(6) Synthesis of $[CdPt_4(PPh_3)_8(\mu_3\text{-}S)_4][ClO_4]_2$ (7). A mixture of **1** (0.150 g, 0.1 mmol) and $Cd(ClO_4)_2$·$7H_2O$(0.025 g, 0.05 mmol) was stirred in MeOH (40 cm^3) for 2 h. The yellow solution was filtered and treated with Et_2O to yield a yellow precipitate, which was purified by recrystallization from CH_2Cl_2/hexane to yield yellow crystals of **7**·$5CH_2Cl_2$·H_2O (**7**) (0.087 g, 46.1%). Anal. Calcd for $C_{144}H_{120}Cl_2CdO_8P_8Pt_4S_4$: C, 52.11; H, 3.62; P, 7.48; S, 3.86. Found: C, 52.54; H, 3.54; P, 7.13; S, 3.67. Λ_m (10^{-3} mol dm^{-3}, CH_2Cl_2, 126.5 Ω^{-1} cm^2 mol^{-1}. $^{31}P\{^1H\}$ NMR (CD_2Cl_2): δ 20.6 ppm [4P, t, ^1J(P−Pt) 3150 Hz], δ 14.8 ppm [4P, t, ^1J(P−Pt) 2995 Hz].

(7) Synthesis of $[ZnPt_4(PPh_3)_8(\mu_3\text{-}S)_4][ClO_4]_2$ (8). A mixture of **1** (0.150 g, 0.1 mmol) and $Zn(ClO_4)_2$·$7H_2O$(0.020 g, 0.05 mmol) was stirred in MeOH (40 cm^3) for 2 h. The yellow solution was filtered and treated with Et_2O to yield a yellow precipitate, which was purified by recrystallization from CH_2Cl_2/hexane to yield yellow crystals of **8** (0.089 g, 52.5%). Anal. Calcd for $C_{144}H_{120}$-$Cl_2ZnO_8P_8Pt_4S_4$: C, 50.93; H, 3.54; P, 7.31; S, 3.77. Found: C, 50.54; H, 3.46; P, 6.78; S, 3.65. Λ_m (10^{-3} mol dm^{-3}, CH_2Cl_2) 128.4 Ω^{-1} cm^2 mol^{-1}. $^{31}P\{^1H\}$ NMR ($CDCl_3$): δ 14.3 ppm [8P, t, ^1J(P−Pt) 3660 Hz].

Crystallography. Single crystals of **2** and **3** suitable for X-ray diffraction studies were grown from CH_2Cl_2/MeOH (1:3) by slow evaporation at room temperature in air. Single crystals of **6** and **7** were from CH_2Cl_2/hexane (1:4) by slow diffusion. Single crystals of **4** and **5** were grown from MeOH by slow evaporation at room temperature in air. The crystals were unstable due to the loss of the solvates upon isolation and were hence sealed in a quartz capillary with the mother liquor during data collection. Data collections of the crystals of complexes **2**−**5** and **7** were carried out on a Siemens CCD SMART system while complex **6** was done on a Siemens *R*3*m*/v diffractometer. Details of crystal and data collection parameters are summarized in Table 3.

The structures of the six complexes were solved by direct methods and difference Fourier maps. Full-matrix least-squares

refinements were carried out with anisotropic temperature factors for all non-hydrogen atoms except for fluorine atoms which were refined isotropically. Hydrogen atoms were placed on calculated positions (C−H 0.96 Å) and assigned isotropic thermal parameters riding on their parent atoms. Calculations were carried out on a Silicon Graphics workstation using the SHELXTL-93 software package.[35] Corrections for absorption were carried out by the SADABS method.

(35) Sheldrick, G. M. *SHELXL-93, Program for Crystal Structure Refinement*; University of Göttingen: Göttingen, Germany, 1993.

Acknowledgment. The authors acknowledge the National University of Singapore (NUS) for financial support. Z.L. and H.L. thank the NUS for a research scholarship award. Technical support from the Department of Chemistry of NUS is appreciated.

Supporting Information Available: X-ray crystallographic files in CIF format for the structure determinations of **2**−**7**. This material is available free of charge via the Internet at http://pubs.acs.org.

IC034884+